Journal of Colloid and Interface Science 418 (2014) 95–102

Contents lists available at ScienceDirect

Journal of Colloid and Interface Science

www.elsevier.com/locate/jcis

A drag reducing surfactant threadlike micelle system with unusual rheological responses to pH

Haifeng Shi [a,1], Wu Ge [a,2], Yi Wang [b], Bo Fang [c], Jacob T. Huggins [a], Tyler A. Russell [a], Yeshayahu Talmon [d], David J. Hart [e], Jacques L. Zakin [a,*]

[a] Department of Chemical and Biomolecular Engineering, The Ohio State University, 140 W 19th Ave, Columbus, OH 43210, USA
[b] Beijing Key Laboratory of Urban Oil and Gas Distribution Technology, China University of Petroleum, Beijing 102249, China
[c] Research Center of Chemical Engineering, East China University of Science and Technology, Shanghai 200237, China
[d] Department of Chemical Engineering, Technion–Israel Institute of Technology, Haifa 32000, Israel
[e] Department of Chemistry, The Ohio State University, Columbus, OH 43210, USA

ARTICLE INFO

Article history:
Received 26 August 2013
Accepted 28 November 2013
Available online 8 December 2013

Keywords:
pH-responsive
Threadlike micelles (TLMs)
Rheology
Drag reduction
Cryo-transmission electron microscopy (Cryo-TEM)
NMR
Zeta potential

ABSTRACT

A pH-responsive threadlike micellar system was developed by mixing alkyl bis(2-hydroxyethyl)methylammonium chloride (EO12) and *trans*-o-coumaric acid (tOCA). The rheological response of this system to pH is unusual in that it has viscoelasticity at both high and low pH levels, while it shows water-like behaviors at medium pH. Cryogenic transmission electron microscopy (Cryo-TEM) images confirmed the presence of TLMs at pH 3.5 and pH 9.8. This system also had DR (drag reduction) capability at low and high pH. The unusual rheological and micellar responses of this system to pH are caused by the dual pK_a's of tOCA. ^{1}H NMR and zeta potential results support this hypothesis.

1. Introduction

In the presence of suitable counterions, cationic surfactants can self-assemble to form threadlike micelles (TLMs) in aqueous solutions, resulting in viscoelastic behaviors [1–7]. Such TLM solutions have been studied extensively for many applications such as oil field applications [8], home-care and personal-care products [9,10], and drag reduction [11–13]. Drag reduction is a striking characteristic of TLMs solutions, which have significantly lower friction loss in turbulent flow than water [11]. The %DR can reach 80% or even higher [7,14,15]. This significant reduction in pressure loss can be utilized in recirculating systems such as district heating/cooling systems [7,11,15–18], to reduce energy consumption for pumping fluids.

Recently, more and more interest has been directed to stimuli-responsive TLMs to develop "smart viscoelastic fluids" [19], whose viscoelasticity can be controlled via external stimuli such as pH [20–29], light [30–36], temperature [37–40], and redox reaction [41]. Among those, pH stimulus is of particular interest since this pH control is relatively easy and reversible. To the best of our knowledge, all the pH-responsive micelle systems [20–29] had characteristics, such as micelle size and rheological behaviors, that either were monotonic functions of pH or had only one peak in the entire pH range. No pH-responsive surfactant-counterion system that shows bimodal rheological and micellar responses to pH has been reported.

Herein, we report a fast pH-responsive surfactant-counterion micelle system that is unique in that it shows viscoelasticity at both low and high pH values. Generally, pH-responsive TLMs systems are formulated by using either pH-responsive surfactant [20–25] or pH-responsive counterions (or hydrotropes) [26–29]. Our TLMs system consists of a cationic surfactant, alkyl bis (2-hydroxyethyl)methylammonium chloride (EO12), and a pH-responsive counterion, *trans*-o-coumaric acid (tOCA), which has dual pK_a's. At low pH, EO12 (4 mM) and tOCA (8 mM) self-assemble into TLMs, which are essential to viscoelastic behavior and drag reducing effectiveness. As pH increases into the medium range, the TLMs aggregate into a separate phase. The resulting two phase system is water-like and is not drag reducing. However, as pH increases to higher levels, the TLMs are dispersed in the solution again, and the solution regains its viscoelasticity and drag reducing

* Corresponding author. Fax: +1 614 292 3769.
E-mail address: zakin.1@osu.edu (J.L. Zakin).
[1] Present address: The Dow Chemical Company, Freeport, TX 77541, USA.
[2] Present address: Mondelēz International, East Hanover, NJ 07936, USA.

0021-9797/$ - see front matter © 2013 Elsevier Inc. All rights reserved.
http://dx.doi.org/10.1016/j.jcis.2013.11.078

ability. The micellar phase behaviors were suggested by rheological properties and demonstrated by cryo-TEM. These unique responses to pH make this solution potentially useful for switchable applications in either acidic or basic environments.

2. Experimental

2.1. Materials

The surfactant used in this pH-responsive system was EO12, donated by Akzo Nobel (commercial name: Ethoquad O/12 PG). It consists of alkyl bis(2-hydroxyethyl)methyl ammonium chlorides (82 wt%) and propylene glycol (18 wt%) as the solvent. The alkyl groups consist of about 82% oleyl (i.e., unsaturated C_{18}), 12% saturated C_{16}, 4% saturated C_{14}, and 1% saturated C_{12}. Scheme 1 shows the structure of the major component, oleyl bis(2-hydroxyethyl)methyl ammonium chloride.

The counterion, tOCA (Scheme 2), with purity greater than 98.0%, was purchased from TCI America. Sodium hydroxide (NaOH) and hydrochloric acid (HCl), diluted as needed, were used to adjust pH of all solutions. NaOH (purity > 98.6%) was purchased from Mallinckrodt Chemicals. HCl (concentration > 73.1%) was purchased from Fisher Scientific.

The threadlike micellar system, 4 mM EO12 + 8 mM tOCA, was prepared by mixing EO12 and tOCA in distilled water followed by stirring for 5 min. pH of the solutions was adjusted by adding 0.5 M NaOH or 0.5 M HCl aqueous solutions. An Oakton pH 11 meter was used to determine the pH.

2.2. Rheology

Rheological experiments were carried out on an ARES rheometer (TA Instruments). Shear viscosity (η) was measured using a Couette tool. The bob of the Couette tool has an 25 mm outer diameter and a 32 mm length and the cup has a 27 mm inner diameter. First normal stress difference ($N1$) was measured using cone and plate. The cone has a 50 mm diameter and an angle of 0.02 radians. The measured $N1$ values need to be corrected for inertial effects according to Macosko [42].

$$N_1^{\text{corrected}} = N_1^{\text{measured}} + 0.15\rho\omega^2R^2 \quad (1)$$

where ρ is the solution density, ω is the angular velocity of the plate and R is the radius of the plate.

For rheological measurements, pH was adjusted and stabilized before experiments. The solution usually reached a stable pH value soon after HCl or NaOH was added. For reversibility experiments, 0.5 M NaOH or 0.5 M HCl were added alternately to 20 mL solution. Since it is difficult to reach exactly the same pH every time, only approximate pH values were obtained. But this does not compromise the reversibility of the rheological responses to pH changes.

Shear viscosity data below shear rates of 15 s^{-1} are not reported here as those data are subject to considerable uncertainty because the surfactant systems are so dilute that the torque at such low shear rates is smaller than the lower limit of the capability of our rheometer. Each rheological measurement was taken right after pH adjustment and completed within 7 min. Since it takes the intermediate pH system at rest typically one hour to form two separate phases, rheological properties measured were for the dispersion of the two phases.

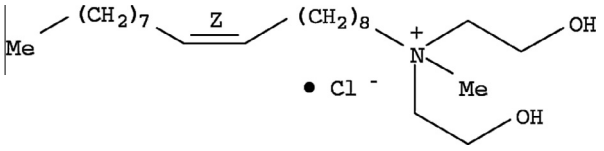

Scheme 1. Molecular structure of oleyl bis(2-hydroxyethyl)methyl ammonium chloride, the major component of cationic surfactant EO12.

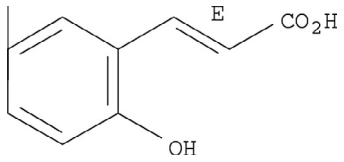

Scheme 2. Molecular structure of counterion *trans*-o-coumaric acid (tOCA).

2.3. Cryo-TEM

Samples for cryo-TEM imaging were prepared at Ohio State University. Cryo-TEM images were taken at the Technion Laboratory for Electron Microscopy of Soft Matter, supported by the Technion Russell Berrie Nanotechnology institute (RBNI). Details of cryo-TEM sample preparation have been described elsewhere [35,43], performed in the Laboratory of Electron Microscopy of Soft Matter.

2.4. Zeta potential

Zeta Potential was measured on a Malvern Instruments Zetasizer Nano-ZS with backscatter detection at 173°. Zeta potential measurements were carried out within 24 h after sample solutions were prepared. Samples were loaded in disposable optical cuvettes with 1 cm path length and equilibrated at 25 °C. The laser wavelength on the instrument was 532 nm. The correlator on the instrument probed times of 500 ns and greater.

2.5. ^1H NMR

Samples for ^{1}H NMR were prepared in D_2O. The oily phase was carefully separated and was dissolved in dimethyl sulfoxide-d_6 (DMSO) before ^{1}H NMR measurements. Experiments were performed at ambient temperature with a Bruker DPX 400 MHz NMR spectrometer in the Department of Chemistry at The Ohio State University.

2.6. Drag reduction

Percent drag reduction (%DR) is defined as

$$\%\text{DR} = \frac{f_{\text{water}} - f}{f_{\text{water}}} \times 100\% \quad (2)$$

where f is the friction factor, defined as

$$f = \frac{\Delta PD}{2\rho LV^2} \quad (3)$$

where ΔP is the pressure drop across the test section of length L, D is the inner diameter of the tube, ρ is the density of the solution, and V is the mean flow velocity.

Drag reduction experiments started from low pH. pH was increased by adding NaOH pellets to the recirculation system. The drag reduction was measured after a stable pH was reached by pumping the solution continuously. Details of the drag reduction experiment are described elsewhere [34].

3. Results and discussion

3.1. Physical appearances

At different pH levels, 4 mM EO12 + 8 mM tOCA solution has different appearances as shown in Fig. 1. The solution at pH 3.6 is colorless, transparent, and recoils when stirring ceases. At pH 6.7, the solution looks cloudy, and behaves like a Newtonian fluid. The suspended micro-drops agglomerate, and eventually form a separate phase. Interestingly, in deuterated water (D_2O), this separated phase is the upper phase, while in H_2O, it is the lower phase. This suggests the oily phase density is between that of D_2O (1.105 g/cm^3) and H_2O (0.998 g/cm^3). At pH 9.7, the separate phase re-dissolves and the solution is transparent again with a greenish tint. The solution regains viscoelastic behavior.

3.2. Rheology

The 4 mM EO12 + 8 mM tOCA solution shows different flow behaviors at different pH levels. At pH 3.6, the solution is viscoelastic and recoils when the stirring ceases, while at pH 6.7, it behaves like a Newtonian fluid. The solution regains viscoelastic behavior at pH 9.7. η and $N1$ of these three samples at 25 °C are shown in Fig. 2. At pH 3.6, η first increases at low shear rates due to the well-known SIS of the TLMs [45–47]. As the shear rate increases over 25 s^{-1}, the solution shows shear-thinning behavior. Its $N1$ has a steep jump in the shear rate range of 25–63 s^{-1} and increases slowly up to 356 Pa at 1000 s^{-1}, indicating the solution is viscoelastic at high shear rates. Although the solution at pH 6.7 also shows shear thinning behavior, suggesting that there might be some particles like globular micelles, no evidence of SIS is observed and the η is significantly lower over the shear rate range of 10–1000 s^{-1}. The absence of SIS and low η indicate that there are barely any TLMs in the solution. In addition, its $N1$ is essentially zero throughout the shear rate range, which also indicates that there are few TLMs present. For the solution at pH 9.7, a strong SIS is observed in the shear rate range of 40–100 s^{-1}. The SIS is followed by shear-thinning behavior, and η is almost the same as that of pH 3.6. Its $N1$ increases steadily with shear rate with a maximum of 465 Pa at 1000 s^{-1}, indicating the presence of TLMs.

Fig. 3 shows the responses of η and $N1$ to pH at the shear rate of 1000 s^{-1}. Both η and $N1$ have two peaks over the pH range of 2–12. As pH increases from 2.6 to 3.6, η and $N1$ increase significantly by over 2 and 8 times respectively and reach their local maxima in the acidic range. They drop quickly as pH increases further and become constant in the medium pH range. As pH increases from 8.7, they again increase significantly by more than 3 and 40 times respectively at pH 9.7 and reach their second local maxima in the basic range. As pH exceeds 9.7, both η and $N1$ fall significantly. The dual viscoelastic behavior over the pH spectrum is unique and makes this pH-responsive micellar solution viscoelastic in either acidic or basic systems, and thus potentially useful in systems that are both acidic and basic at different times or locations.

Real applications may require that viscoelasticity can be reversibly switched on and off many times. The rheological responses to pH were tested for 5 cycles of pH changes. Fig. 4 shows that the high η at low pH is reduced at medium pH and is increased at high pH. Even after 5 cycles of pH changes the reversible changes in η are still effective with no significant decay. Similar results for $N1$ were also observed (see Supporting materials).

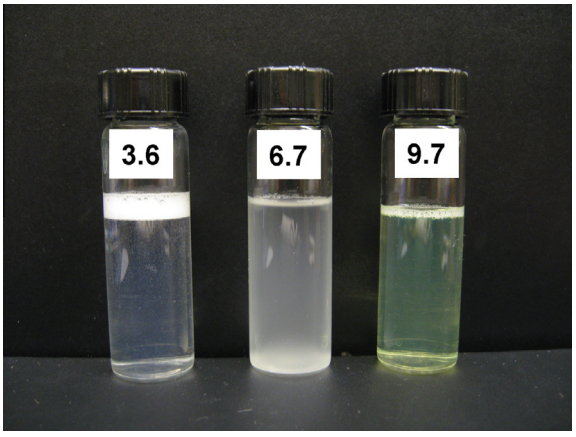

Fig. 1. Appearances of 4 mM EO12 + 8 mM tOCA solution in vials at pH = 3.6 (left), 6.7 (middle) and 9.7 (right).

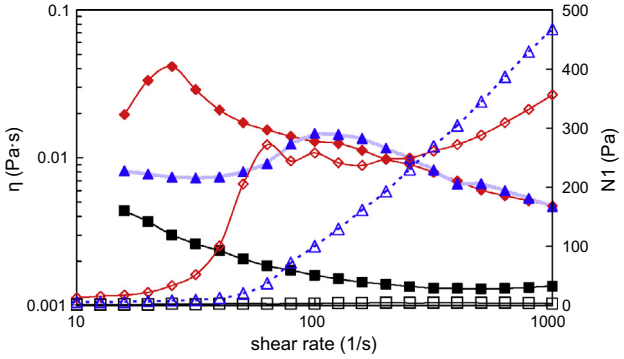

Fig. 2. η and $N1$ of 4 mM EO12 + 8 mM tOCA at different pH against shear rate at 25 °C. (Diamonds: pH = 3.6, squares: pH = 6.7, triangles: pH = 9.7. Solid symbols: η, open symbols: $N1$).

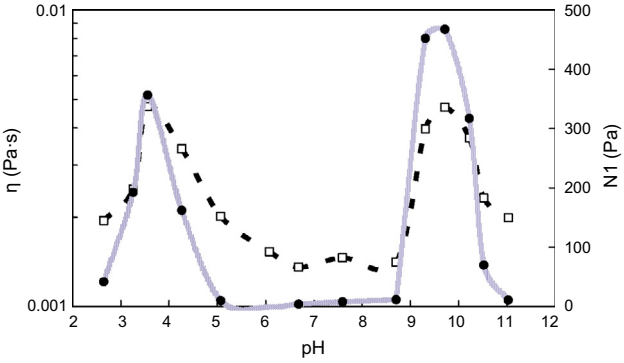

Fig. 3. η and $N1$ of 4 mM EO12 + 8 mM tOCA at shear rate of 1000 s^{-1} against pH at 25 °C. (open squares: η, solid circles: $N1$).

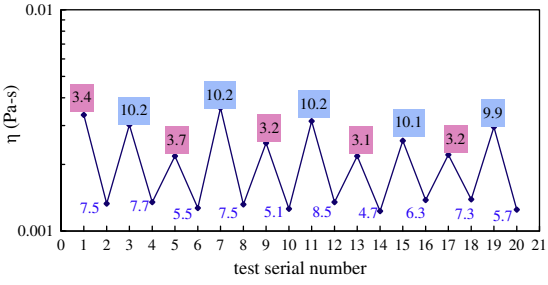

Fig. 4. η of 4 mM EO12 + 8 mM tOCA at shear rate 1000 s^{-1} against pH cycles at 25 °C. (pH values are indicated near each data point).

3.3. Cryo-TEM

It is well known that TLMs can induce viscoelasticity as they entangle under shear. So the changes in viscoelasticity correspond to the changes in TLMs. At low and high pH levels, EO12 binds with tOCA and forms TLMs. However, at medium pH level, the TLMs agglomerate and form the dispersed insoluble phase, which eventually separates out. Cryo-TEM images of the nanostructures of the 4 mM EO12 + 8 mM tOCA solution at different pH levels are shown in Fig. 5. At pH 3.5, randomly curled TLMs permeate evenly throughout the solution. The micelles are long and inter-connecting with each other. In fact, no free ends of the TLMs can be found in the cryo-TEM image. These TLMs do not aggregate and thus make the solution a stable colloidal system. At pH 5.5, however, no TLMs are present. Instead, only very large aggregates like membrane sheets are observed. These large aggregates make the colloidal system cloudy and form a separate phase eventually. At pH 8.0, micelles show up again. The cryo-TEM image shows a lamellar structure (onion-like structure). Numerous micelles are wrapped up by a number of layers. One can hardly tell the shape of the micelles. They are probably TLMs encompassed by the lamellar structure. The structures at pH 8.0 are definitely different from those at pH 5.5, and they form a dispersed phase in the solution and also make the solution cloudy. At pH 9.8, well developed TLMs are observed. They are randomly curled and evenly distributed in the solution. The micelles are long and inter-connecting with each other with no free ends observed. The η and $N1$ at pH 9.8 are generally larger than the low pH peaks commensurate with the large TLMs. Interestingly, a closed loop micelle is also observed close to the center of the image (see arrow in Fig. 5). Since these TLMs are evenly distributed in the solution, they stabilize the solution, forming a transparent colloidal system.

The cryo-TEM images indicate that the state of TLMs, dispersed or flocculated, is critical to the physical appearances and rheological properties of the solution. As has been explained in the literature [11,13,26], the formation of TLMs is caused by strong hydrophobic interactions between the surfactant's "tail" and the counterion's aromatic part. The question is what determines the TLMs' state. In general, electrostatic forces are likely to play an important role in this process. At low pH, TLMs carry positive charge, which cause repulsive electrostatic forces among the TLMs. The repulsive electrostatic forces prevent TLMs from agglomerating. At medium pH, TLMs carry little or zero charge, resulting in little or no repulsive electrostatic forces among the TLMs. As a result, the TLMs agglomerate and form precipitation. At high pH, TLMs carry negative charge, which also cause repulsive electrostatic forces among the TLMs. As a result, the TLMs cannot agglomerate and stay dispersed in the aqueous system. The charge on TLMs depends on the different dissociation levels of tOCA at different pH levels.

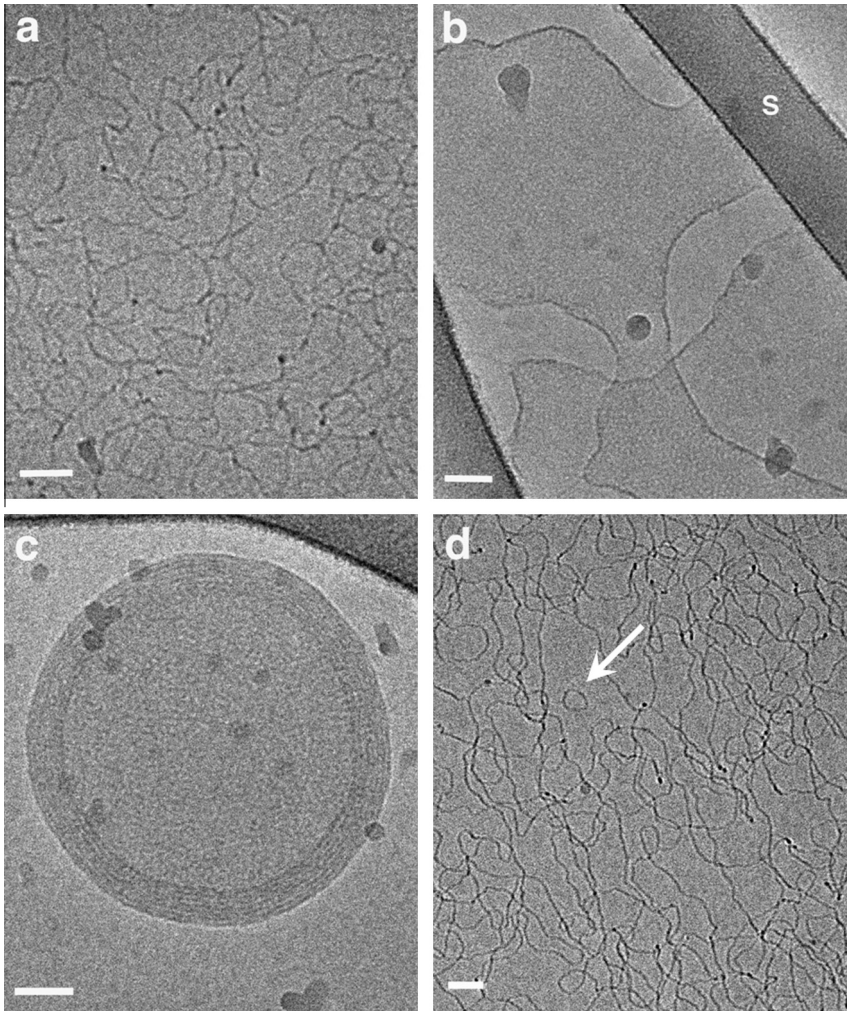

Fig. 5. Cryo-TEM images of 4 mM EO12 + 8 mM tOCA at different pH. (a) pH = 3.5, (b) pH = 5.5, (c) pH = 8.0, (d) pH = 9.8. 'S' in (b) denotes the support film. All scale-bars correspond to 50 nm. Arrow in (d): a closed loop micelle.

This mechanism is further explained in Fig. 6. The tOCA has dual pK_a's; 4.5 for the carboxylic group and 9.6 for the hydroxyl group. At pH lower than 4.5, the majority of tOCA molecules are not dissociated and carry zero charge. When these zero-charged tOCA molecules combine with EO12 molecules, which carry one positive charge, the resulting TLMs have a positive net charge, which prevents the agglomeration of neighboring TLMs due to the electrostatic repulsion. When pH increases to the medium level, the carboxylic group on the majority of the tOCA molecules is dissociated, resulting in one negative charge on the tOCA molecules. If tOCA combines with EO12 at 1:1 M ratio, these negatively charged tOCA molecules, in turn, neutralize the positively charged EO12 molecules, resulting in the flocculation of TLMs. As pH further increases, the hydroxyl group begins to dissociate, making TLMs negatively charged and they re-disperse in the solution.

3.4. Zeta potential

The magnitude of zeta potential can be used to evaluate the potential stability of the colloidal system. Since zeta potential is the potential at the slipping plane of a particle, it reflects the sign of the charge the particle carries. With large negative or positive zeta potential, particles tend to repel each other and stay dispersed stably in the system. But if the zeta potential has low values, the electrostatic repulsion is not strong enough to prevent the flocculation of the particles. Zeta potentials for the 4 mM EO12 + 8 mM tOCA solution at different pH levels are shown in Fig. 7. Zeta potential generally decreases as pH increases. The zeta potential has its greatest value of 33 mV at pH 3.6. At pH 8.7, it declined to zero. As pH increases further, the decrease in zeta potential is not significant, and it levels off to its lowest value of −4.5 at pH 10.5. The results show that the micelles carry positive charge at low pH and negative charge at high pH. It also helps to explain the stable dispersion of TLMs due to strong electrostatic repulsion at low pH and the flocculation of TLMs and the observed phase separation due to the weak electrostatic repulsion at the medium pH level. At pH = 9.8, the zeta potential is −3.8 mV, which should not be able to prevent the TLMs from flocculating. One explanation is that the zeta potential cannot be correctly obtained as the solution at high pH has a green color, which coincides with the color of the laser (532 nm) of the Zetasizer instrument. The stable dispersion of TLMs at high pH might also be maintained by other effects, for example, steric effects, in addition to the electrostatic repulsion.

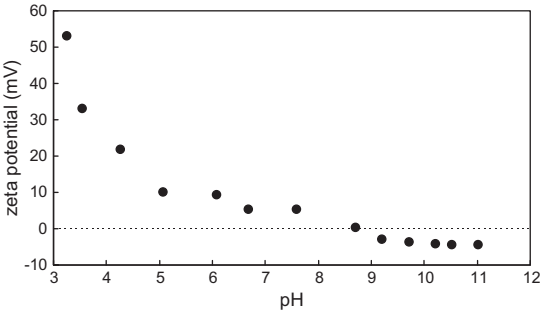

Fig. 7. Zeta potential of 4 mM EO12 + 8 mM tOCA against pH at 25 °C.

This low positive zeta potential phenomenon in a stable colloidal system was also observed by Ge et al. [7].

3.5. ^{1}H NMR

The proposed mechanism above has one assumption, which is that tOCA and EO12 combine at a 1:1 M ratio when the TLMs flocculate and form a separate phase. This ratio can be extracted from ^{1}H NMR spectra. The two separated phases of solution at pH 6.6 were analyzed by ^{1}H NMR. Fig. 8 is the ^{1}H NMR spectrum of the oily phase of 4 mM EO12 + 8 mM tOCA at pH 6.6. Peaks of both tOCA and EO12 appear in the spectrum. The peak group on the left end corresponds to the two hydrogen atoms on positions a and b of tOCA as noted on the figure. The peak area is set at 1.00. Peak "c" is one of the EO12 peaks. It corresponds to the two hydrogen atoms on the second carbon from the nitrogen atom on the long alkyl chain. The peak area is 1.02, which is very close to the peak area of tOCA's hydrogen atoms at positions a and b, showing that the molar ratio of tOCA to EO12 is essentially 1:1. It should be noted that some other peaks of EO12 do not reflect the same ratio as EO12 has mixed alkyl groups.

Fig. 9 is the ^{1}H NMR spectrum of the D_2O phase of 4 mM EO12 + 8 mM tOCA at pH 6.6. In the high ppm region, tOCA peaks are observed. On the other hand, no EO12 peaks were observed in the low ppm region. Only peaks for propylene glycol, which is the solvent for EO12, are observed. This NMR spectrum shows that there are no EO12 molecules dissolved in the D_2O phase, which means all EO12 molecules go into the separated oily phase with tOCA. Since the starting concentration of tOCA is 8 mM, twice the

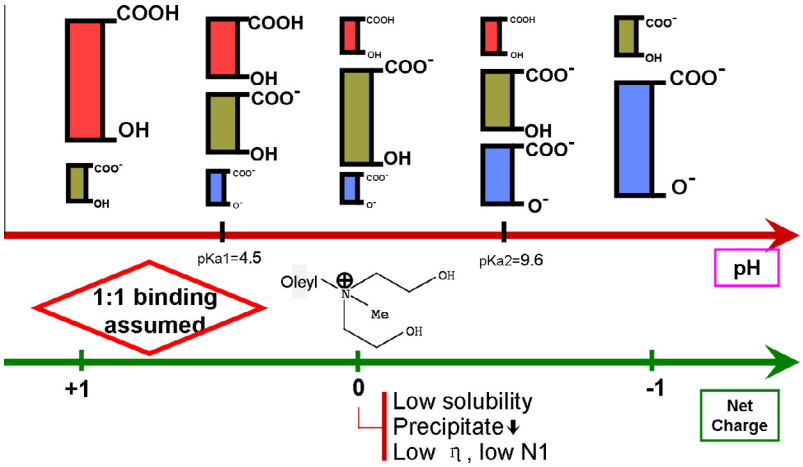

Fig. 6. Proposed mechanism based on electrostatics. The colored rectangles with function groups represent tOCA molecules. Different color represents tOCA with different numbers of charges. And the size corresponds to their relative concentration. (For interpretation of the references to color in this figure legend, the reader is referred to the web version of this article.)

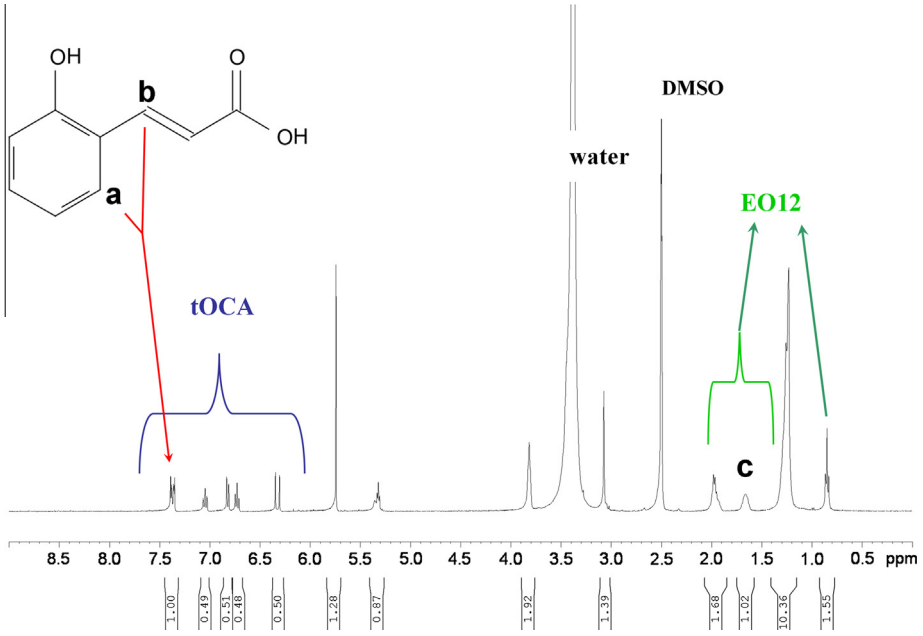

Fig. 8. ^{1}H NMR spectrum of the oily phase of 4 mM EO12 + 8 mM tOCA at pH 6.6.

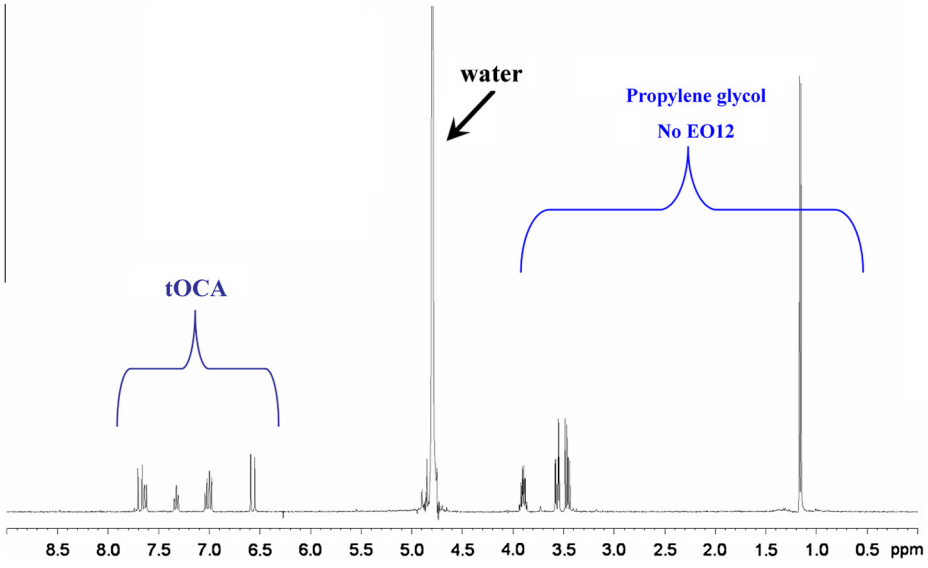

Fig. 9. ^{1}H NMR spectrum of the D_2O phase of 4 mM EO12 + 8 mM tOCA at pH 6.6.

concentration of EO12, it is reasonable that excess tOCA should remain in the D_2O phase and tOCA and EO12 form the separate oily phase at 1:1 M ratio.

3.6. Drag reduction

Surprisingly, few studies of the pH effects on drag reduction of surfactant micelle solutions have been reported. Chou [44] found that the drag reduction of a cationic surfactant solution containing either phthalate or isophthalate as counterion increased as the pH decreased. The dependence was due to ionization of both carboxyl groups on the phthalates isomers at high pH level. Herein, the effects of pH on drag reduction capability of EO12 + tOCA were studied at two concentrations (4 mM/8 mM and 2.7 mM/5.4 mM) and at two temperatures (10 °C and 20 °C).

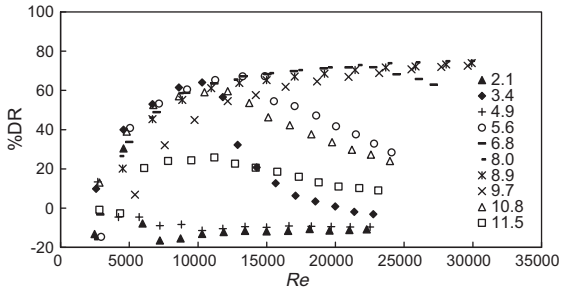

Fig. 10. Drag reduction of the solution 2.7 mM EO12 + 5.4 mM tOCA at different pH at 10 °C. (*Re* is based on the solvent viscosity).

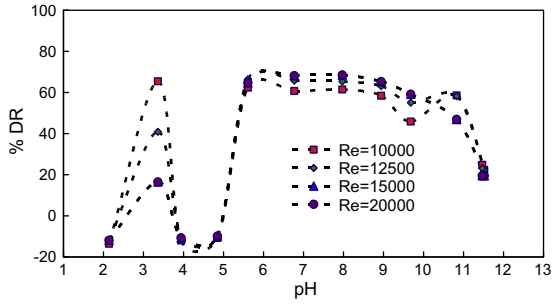

Fig. 11. Drag reduction of the solution 2.7 mM EO12 + 5.4 mM tOCA against pH for different Re at 10 °C. (*Re* is based on the solvent viscosity).

Fig. 10 shows the drag reduction of the solution of 2.7 mM EO12 + 5.4 mM tOCA at different pH levels at 10 °C. At pH 2.1, the solution is not drag reducing and has greater resistance to flow than water. When pH increases to 3.4, the solution shows increasing drag reduction capability and reaches a maximum value of 62% at *Re* of 8500. It loses drag reduction capability sharply as *Re* exceeds 8500 indicating only modest resistance to shear. At pH 4.9, the solution loses its drag reduction capability completely. As pH increases to the range of 5.6–6.8, the drag reduction capability improves. It reaches a maximum in the pH range of 8.0–9.7. Drag reduction capability reaches high values at *Re* of 10,000, and maintains 70% as *Re* increases to the maximum values the experiment can reach. As pH further increases to 10.8 and to 11.5, the drag reduction capability decreased gradually. %DR has a maximum value of 60% at *Re* of 12,000 and 25% at *Re* of 11,000 at pH 10.8 and 11.5 respectively.

The dependence of drag reduction on pH is shown in Fig. 11, which shows the drag reduction of the 2.7 mM EO12 + 5.4 mM tOCA solution against pH for different *Re* at 10 °C. Generally, the solution has two drag reduction effective regions through the entire pH range. In the pH range of 3.9–4.9, the drag reduction capability has a gap. In the pH range of 2.1–3.9, the solution shows high drag reduction capability at lower *Re*. The low drag reduction values at high *Re* are because of mechanical shear degradation. However, when the solution is drag reducing at pH above 5.0, its drag reduction capability increases slowly with *Re*.

Additional drag reduction results can be found in the Supporting materials. Generally, for the solution of 4 mM EO12 + 8 mM tOCA, the drag reduction capability has two effective regions through the entire pH range at 10 °C. However, there is no significant drag reduction gap at 20 °C. For the 2.7 mM EO12 + 5.4 mM tOCA solution, the drag reduction capability has two effective pH regions at both 10 °C and 20 °C (data not shown). The drag reduction gap is on the low pH side for the solution of 2.7 mM EO12 + 5.4 mM tOCA (Fig. 11), while it is at a high pH value for the solution of 4 mM EO12 + 8 mM tOCA at 10 °C (see Fig. S3 in Supporting materials).

4. Conclusions

The 4 mM EO12 + 8 mM tOCA solution is pH-responsive. The rheological responses of this system to pH are unique in that it has viscoelasticity at both low and high pH levels. The viscoelasticity changes are induced by the morphological changes of TLMs as observed in cryo-TEM images. The solution is viscoelastic when the TLMs are well dispersed, but it loses viscoelasticity and has phase separation when the TLMs flocculate at medium pH. The TLMs' behavior is dependent on pH, because TLMs have different electric charges at different pH levels as suggested by zeta potentials. The difference in electric charges of TLMs stems from the dual pK_a's of the counterion tOCA, as tOCA carries different charges at different pH. When it combines with EO12 at 1:1 M ratio, the net charge of the TLMs varies from −1 to 0 and 0 to +1. When the net charge is non-zero, it generates repulsion between neighboring TLMs and prevents them from flocculating, giving a stable colloid with viscoelastic behavior. The 1:1 M ratio of EO12 to tOCA in the separated oily phase was confirmed by ^{1}H NMR spectra. The solution of two concentrations at two temperatures shows two drag reduction regions over the entire pH range. The discrepancy between drag reduction capability and viscoelasticity might be caused by drag reduction effects induced by deformed particles of the oily phase dispersed by high shear stress and turbulent movements of the fluid. Our work not only broadened the pH range of studies on pH-responsive TLMs [25,26,29], but also provided a bimodal pH-responsive TLMs system that can be used in either basic or acidic applications where viscoelasticity is controlled by pH. The proposed mechanism explained the unique bimodal rheological behaviors successfully. It also suggests that there are probably similar systems that have more than two peaks of rheological behaviors over a pH range if multiple counterions with different pK_a's are used.

Acknowledgments

This work was financially supported by a Presidential Fellowship awarded to H. Shi from The Ohio State University and by National Natural Science Foundation of China (51206186). Thanks to Dr. Ellina Kesselman and Ms. Judith Schmidt for their help with cryo-TEM experiments.

Appendix A. Supplementary material

Supplementary data associated with this article can be found, in the online version, at http://dx.doi.org/10.1016/j.jcis.2013.11.078.

References

[1] T. Shikata, Y. Sakaiguchi, H. Uragami, A. Tamura, H. Hirata, J. Colloid Interface Sci. 119 (1987) 291.
[2] T.M. Clausen, P.K. Vinson, J.R. Minter, H.T. Davis, Y. Talmon, W.G. Miller, J. Phys. Chem. 96 (1992) 474.
[3] P.A. Hassan, J.V. Yakhmi, Langmuir 16 (2000) 7187.
[4] S. Imai, T. Shikata, J. Colloid Interface Sci. 244 (2001) 399.
[5] L.M. Walker, Curr. Opin. Colloid Interface Sci. 6 (2001) 451.
[6] P.A. Hassan, S.R. Raghavan, E.W. Kaler, Langmuir 18 (2002) 2543.
[7] W. Ge, E. Kesselman, Y. Talmon, D.J. Hart, J.L. Zakin, J. Non-Newtonian Fluid Mech. 154 (2008) 1.
[8] T. Hughes, E. Nelson, P. Sullivan, V. Anderson, in: R. Zana, E.W. Kaler (Eds.), Giant Micelles, CRC Press, New York, 2007, p. 453.
[9] L. Nicolas-Morgantini, in: R. Zana, E.W. Kaler (Eds.), Giant Micelles, CRC Press, New York, 2007, p. 493.
[10] S. Ezrahi, A. Aserin, N. Garti, E. Tuval, in: R. Zana, E.W. Kaler (Eds.), Giant Micelles, CRC Press, New York, 2007, p. 515.
[11] J.L. Zakin, B. Lu, H. Bewersdorff, Rev. Chem. Eng. 14 (1998) 253.
[12] W. Ge, Y. Zhang, J.L. Zakin, Exp. Fluids 42 (2007) 459.
[13] W. Ge, H. Shi, Y. Talmon, D.J. Hart, J.L. Zakin, J. Phys. Chem. B 115 (2011) 5939.
[14] W.I.A. Aly, H. Inaba, N. Haruki, A. Horibe, J. Heat Transfer 128 (2006) 800.
[15] H. Shi, Y. Wang, B. Fang, J.T. Huggins, T.R. Huber, J.L. Zakin, Adv. Mech. Eng. (2011), http://dx.doi.org/10.1155/2011/315943.
[16] K. Gasljevic, E.F. Matthys, Energy Build. 20 (1993) 45.
[17] J. Yang, Curr. Opin. Colloid Interface Sci. 7 (2002) 276.
[18] A. Krope, L.C. Lipus, Appl. Therm. Eng. 30 (2010) 833.
[19] F.P.J. Hubbard, N.L. Abbott, in: R. Zana, E.W. Kaler (Eds.), Giant Micelles, CRC Press, 2007, p. 375.
[20] H. Kawasaki, M. Souda, S. Tanaka, J. Phys. Chem. B 106 (2002) 1524.
[21] M. Johnsson, A. Wagenaar, M.C.A. Stuart, J.B.F.N. Engberts, Langmuir 19 (2003) 4609.
[22] H. Maeda, S. Tanaka, Y. Ono, J. Phys. Chem. B 110 (2006) 12451.
[23] M. Scarzello, J.E. Klijn, A. Wagenaar, Langmuir 22 (2006) 2558.
[24] J.E. Klijn, M.C.A. Stuart, M. Scarzello, A. Wagenaar, J.B.F.N. Engberts, J. Phys. Chem. B 111 (2007) 5204.
[25] Y. Zhang, Y. Han, Z. Chua, S. He, J. Zhang, Y. Feng, J. Colloid Interface Sci. 394 (2013) 319.
[26] Y. Lin, X. Han, J. Huang, J. Colloid Interface Sci. 330 (2009) 449.

[27] G. Verma, V.K. Aswal, P. Hassan, Soft Matter 5 (2009) 2919.
[28] M. Ali, M. Jha, S.K. Das, S.K. Saha, J. Phys. Chem. B 113 (2009) 15563.
[29] Z.L. Chu, Y.J. Feng, Chem. Commun. 46 (2010) 9028.
[30] H. Sakai, Y. Orihara, H. Kodashima, J. Am. Chem. Soc. 127 (2005) 13454.
[31] A.M. Ketner, R. Kumar, T.S. Davies, P.W. Elder, S.R. Raghavan, J. Am. Chem. Soc. 129 (2007) 1553.
[32] R. Kumar, A.M. Ketner, S.R. Raghavan, Langmuir 26 (2010) 5405.
[33] M. Pereira, C.R. Leal, A.J. Parola, Langmuir 26 (2010) 16715.
[34] H. Shi, Y. Wang, B. Fang, Y. Talmon, W. Ge, S.R. Raghavan, J.L. Zakin, Langmuir 27 (2011) 5806.
[35] H. Shi, W. Ge, H. Oh, S.M. Pattison, J.T. Huggins, Y. Talmon, D.J. Hart, S.R. Raghavan, J.L. Zakin, Langmuir 29 (2013) 102.
[36] H. Oh, A.M. Ketner, R. Heymann, E. Kesselman, D. Danino, D. Falvey, S.R. Raghavan, Soft Matter 9 (2013) 5025.
[37] P.A. Hassan, B.S. Valaulikar, C. Manohar, Langmuir 12 (1996) 4350.
[38] R.T. Buwalda, M.C.A. Stuart, J.B.F.N. Engberts, Langmuir 16 (2000) 6780.
[39] H. Yin, Z. Zhou, J. Huang, Angew. Chem. 115 (2003) 2238.
[40] T.S. Davies, A.M. Ketner, S.R. Raghavan, J. Am. Chem. Soc. 128 (2006) 6669.
[41] K. Tsuchiya, Y. Orihara, Y. Kondo, J. Am. Chem. Soc. 126 (2004) 12282.
[42] C.W. Macosko, In Rheology: Principles, Measurements, and Applications, VCH, New York, 1994.
[43] Y. Talmon, in: R. Zana, E.W. Kaler (Eds.), Giant Micelles, CRC Press, New York, 2007, p. 163.
[44] L.C. Chou, Drag-Reducing Cationic Surfactant Solutions for District Heating and Cooling Systems, Ph.D. Disseration, The Ohio State University, 1991.
[45] H. Wunderlich, H. Hoffmann, Rheol. Acta 26 (1987) 532.
[46] D. Ohlendorf, W. Interthal, H. Hoffmann, Rheol. Acta 25 (1986) 468.
[47] R. Oda, P. Panizza, M. Schmutz, Langmuir 13 (1997) 6407.